Chapter 5

A composite prepared from MoS_2 quantum dots and silver nanoparticles and stimulated by mercury(II) is a robust oxidase mimetic for use in visual detection of cysteine

5.1. Introduction

L-cysteine (Cys), homocysteine, and glutathione are three important biological thiols that have great significance in myriad biological processes and are important products in many areas such as food, cosmetic, and pharmaceutical industries [Pan et al., 2017; He et al., 2019]. Cys being a semi-essential amino acid is an indispensable component of biological fluids. Any discrepancy in Cys level due to oxidative stress, bacterial infections, and other diseases may result in aberrations such as hematopoiesis or psoriasis, hair decolorizations, liver, skin diseases, and even other cardiac or vascular diseases [Xue et al., 2018; Wu et al., 2016]. Therefore, it becomes essential to monitor Cys level in the biological fluids for the medical diagnosis. So far, different strategies established for its detection are fluorescence spectroscopy [Meng et al., 2007], high-performance liquid chromatography [Chwatko et al., 2014], gas chromatography [Menestrina et al., 2016], electrochemical methods [Pazalja et al., 2016; Lee et al., 2015], etc. These methods demand skilled person along with expensive, multi-step sampling or sophisticated instrumentation deterring them from practical implementation. This essentially calls for an economic, environmental, and user-friendly sensing technique for which colorimetric detection method best fits into the framework. It is a well-established and economic method that has emerged that enables quick, unaided naked eye detection of various biomolecules at ultra-trace levels in real samples with remarkable progress [Xue et al., 2018; Wu et al., 2016].

In the past few years, optical sensors developed for Cys detection employing artificial enzymes (nanozyme) that can mimic the natural enzyme like HRP (horse radish peroxidase) mimetic activity [Wu et al., 2016, Xue et al., 2019; Wu et al., 2014; Singh et al., 2017]. Natural enzymes, due to their denaturation, expensive preparations, low recyclability, and low operational stability prompted the scientists towards the synthesis of artificial enzymes [Wu et al., 2013]. In this regard, many successful efforts for synthesis of metal-based nanoparticles, possesing surface plasmon properties such as gold (Au) [Han et al., 2017; Zarlaida et al., 2017; Zhou et al., 2014; Jazayeri et al., 2018], platinum (Pt) [Chen et al., 2016; Lin et al., 2015], silver (Ag)[Jiang et al., 2012; Li et al., 2015; Rameshkumar et al., 2013], etc. as nanozyme for colorimetric detection of various biomolecules and heavy metal ions have received much attention [Lin et al., 2014]. Amongst them, the least attention has been drawn towards AgNPs as they are easily susceptible to chemical degradation, surface oxidation in the aqueous medium, and lower stability. However, a 100-fold greater molar extinction coefficient of AgNPs than AuNPs grabs attention towards the attainment of enhanced sensitivity in optical determination with improved visibility differences [Lin et al., 2014; He et al., 2010; Wang et al., 2010]. This motivated us to find a quick and cheap synthesis for the silver-based nanozyme. Molybdenum disulfide (MoS_2) has discovered a separate space due to its high catalytic, electrical conductivity with significant biocompatibility. In comparison to other MoS_2 nanostructures, MoS_2-QDs have been tremendously applied in various areas like electronics (FETs, Photodetectors, etc.) and biomedical applications (biosensors, bio-imaging, etc.) due to their remarkable optical and electronic properties [Dong et al., 2016; Kufer et al., 2015].

Earlier reports on AgNPs (when taken alone) as nanozyme for mimetic activity have mostly compromised the stability and catalytic efficiency [Mandal et al., 2001]. In response to the above issues, we present a system consisting of MoS_2 quantum dots (MoS_2-QDs) stabilized AgNPs (MoS_2-QDs-AgNPs) with enhanced stability and excellent oxidase activity in presence of mercury(II) (Hg^{2+}) ion for the colorimetric detection of Cys. In the present system, MoS_2-QDs synthesized via hydrothermal process, play the dual role of reducing agent as well as a stabilizer by anchoring themselves via sulphur atom on the surface of AgNPs and thus facilitating the enhancement in oxidase mimetic activity by assisting Ag-Hg amalgam formation. Our reported procedure relieves us from extra ion impurities and highly corrosive H_2O_2 giving MoS_2-QDs-AgNPs with long-term stability (4 weeks) with no signature of aggregation.

Herein, the present study deals with MoS_2-QDs-AgNPs interaction with Hg^{2+} resulting in the formation of Ag-Hg amalgam thereby boosting its oxidase mimetic activity [30]. Ag-Hg interactions have been verified experimentally and through various characterization techniques like TEM, and XPS. Further, Hg^{2+} stimulated oxidase activity has been further exploited for the development of the colorimetric sensing platform for Cys. Cys exhibits an inhibitory effect on the oxidase mimetic activity of the nanohybrid system thus producing visual color contrast based on its different concentrations studied. These results are easily analyzed visually due to the high color contrast of pre-loaded chromogenic substrates (TMB) produced within 2 min. Based on this, we have developed plastic tubes portable kit with corresponding color (wheel) scale that can aid in immediate colorimetric sensing of Cys level in real samples without the use of any sophisticated instrumentation. These pre-loaded MoS_2-QDs-AgNPs-TMB

kits were tested for multiple days and found to be active for up to 5 days exhibiting similar visual differences.

5.2. Experimental

5.2.1. Materials

Sodium molybdate ($Na_2MoO_4.2H_2O$) and L-Cysteine (Cys) ($HO_2CCH(NH_2)CH_2SH$) were purchased from Sisco Research Laboratories (https://www.srlchem.com/). Mercury(II) chloride was purchased from spectrochem (https://spectrochem.in/), silver nitrate, 3,3',5,5'-tetramethylbenzidine (TMB), acetic acid, Homocysteine (HCys) and sodium acetate were purchased from Sigma Aldrich (https://www.sigmaaldrich.com). Amino acids including Cys, L-Alanine (Ala), L-Glycine (Gly), L-Glutamic acid (Glu), L-Aspartic acid (Asp), L-Proline (Pro), L-Tryptophan (Try), L-Methionine (Met), L-Histidine (His), L-Lysine (Lys) and L-Serine (Ser) were purchased from CDH Fine chemical India (https://www.cdhfinechemical.com/). Human blood serum was collected from Prof. D. Das Lab, IMS, BHU, Varanasi. Milli-Q water (resistivity=18.0 MΩ, pH=7) was used in all experiments.

5.2.2. Instrumentation/characterization techniques

Hydrothermal reactor for MoS_2-QDs synthesis was of Hydroion Scientific Instrument Co. Ltd. TEM micrographs of drop casted MoS_2-QDs and MoS_2-QDs-AgNPs were investigated on FEI, TECHNAI G^2 20 TWIN (Czech Republic) TEM instrument, at accelerating voltage of 200 kV. Absorptions spectra of MoS_2-QDs-AgNPs enzyme mimetic activity were investigated on a UV-Vis spectrophotometer (UV-2600, Shimadzu). X-ray photoelectron spectroscopy (XPS) was recorded on Kratos analytical instrument (Shimadzu, Amicus XPS, UK) equipped with MgKα (λ=1.254 Å) radiation.

5.2.3. Synthesis of MoS_2 Quantum dots (MoS_2-QDs)

MoS_2-QDs were synthesized via a one-step hydrothermal route as per earlier report [Mishra et al., 2017; Vinita et al., 2018]. MoS_2-QDs are synthesized through one step hydrothermal route with sodium molybdate ($Na_2MoO_4.2H_2O$) (0.25 g) and L-cysteine ($HO_2CCH(NH_2)CH_2SH$) (0.5 g) as precursors. These are dissolved in 25 ml of Milli-Q water in two separate beakers and kept on ultrasonication for 15 min. The two solutions are mixed slowly with vigorous stirring maintaining 40°C temperature and pH=3.0, respectively. The mixture was then transferred into stainless steel lined Teflon autoclave and left to proceed for 42 hours maintained at ~200°C. Thus, obtained solution is cooled to room temperature naturally and filtered through a microporous membrane; the filtrate is further purified through dialysis in deionized water and further used for AgNPs synthesis.

5.2.4. Synthesis of MoS_2 QDs stabilized Silver nanoparticles (MoS_2-QDs-AgNPs)

Further, synthesized MoS_2-QDs were utilized for the synthesis and stabilization of AgNPs yielding a MoS_2-QDs-AgNPs nanohybrid system. MoS_2-QDs (100 µL) were added dropwise to an aqueous solution of $AgNO_3$ (1.0 mM; 10 mL) in a conical flask kept in a water bath (at 70°C) with continuous stirring at 1000 rpm for 15 min. The dark yellow color obtained AgNPs were stored in dark at low temperature and characterized via TEM for its size distribution. MoS_2-QDs acting as the reducing agent is responsible for the conversion of Ag (I) to Ag (0) state and at the same time serve as a stabilizing agent to obtain a stable hydrosol.

5.2.5. Investigation of Oxidase mimetic activity of MoS_2-QDs-AgNPs stimulated by Hg^{2+}

The oxidase activity of MoS_2-QDs-AgNPs stimulated by Hg^{2+} was investigated in the aqueous medium. In this study, (A) Hg^{2+} (10 µL; 1 mM), (B) TMB (100 µL; 1mM) and (C) MoS_2-QDs-AgNPs (10 uL), D=Cys (100 µL; 50 µM) were taken in ELISA plate with different combinations marked as (a) A+B, (b) A+B+C, (c) B+C, (d) A+B+C+D for recording absorbance spectra.

5.2.6. Colorimetric assay of L-Cysteine detection

Colorimetric sensing of Cys was performed to investigate the oxidase activity of MoS_2-QDs-AgNPs towards TMB oxidation with varying Cys concentration. In a typical experiment, acetate buffer of pH=4.0 (0.2 M, 100 µL), Hg^{2+} (10 µL), Cys (1µM to 100 µM) and MoS_2-QDs-AgNPs (10 µL) solution were mixed in plastic tubes. To the above mixture, TMB (1mM, 100 µL) was added. The mixture content was then transferred to 96-well ELISA plate after color development for recording the absorption spectrum and endpoint (λ=652 nm) each time.

5.2.7. Interference study

Interference from various amino acids was investigated keeping their concentration up to 1mM. MoS_2-QDs-AgNPs (10 µL) solution, Hg^{2+} (10 µL; 1 mM), and acetate buffer (0.2 M, 100 µL) were added to all the above samples stepwise followed by the addition of TMB (100 µL; 1 mM) in order to study the mimetic activity via visible color differences. Their endpoint spectra (λ=652 nm) were recorded and compared with 10 times diluted Cys concentration (100 µM) to investigate the MoS_2-QDs-AgNPs nanozyme activity towards various amino acids. Interferences from the thiol group

containing molecules like glutathione and homocysteine were also investigated in the same concentration range (100μM).

5.3. Results and Discussion

5.3.1. Materials Characterization

MoS_2-QDs prepared via hydrothermal route was well characterized and then further utilized for MoS_2-QDs-AgNPs nanohybrid system formation and its stabilization. TEM micrographs of MoS_2-QDs (Figure 5.1a & b) reveal its uniform dispersion as well as highly ordered and parallel lattice fringes (d=0.27 nm) are visible which is in agreement with the reported works of literature [Mishra et al., 2017; Gopalakrishnan et al., 2014]. SAED pattern shown in Figure 5.1c also confirms its formatiom and crystalline nature [Bai et al., 2017]. Further, size distribution analysis reveals its mean particle size of 5.9±1.1nm (Figure 5.1 d). UV-Vis spectrum (real picture of MoS_2-QDs in inset) (Figure 5.2a), its elemental analysis by EDX (Figure 5.2 b).

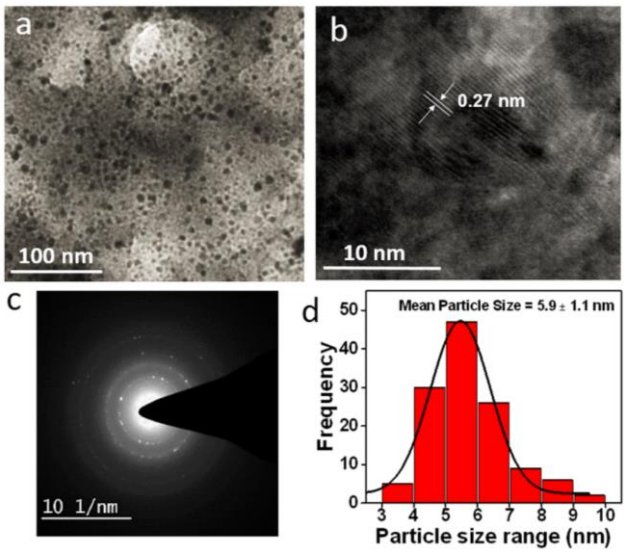

Figure 5.1 Characterization of MoS_2-QDs. TEM micrograph (a) at 100 nm scale bar (b) at higher resolution (10 nm) (arrows indicating lattice fringe spacing) (c) SAED pattern (d) Histogram depicting size distribution.

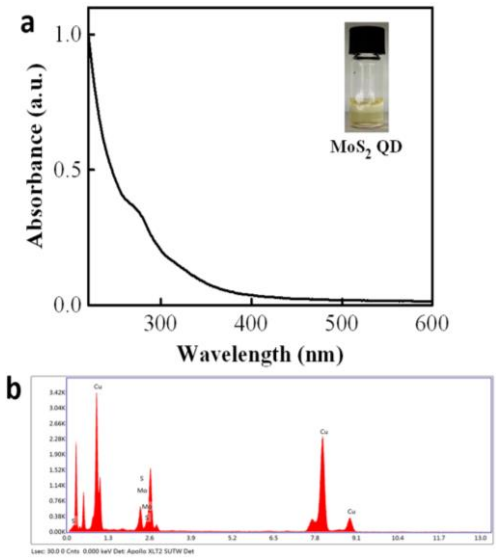

Figure 5.2. (a) UV-Vis spectra and (b) EDS spectrum of MoS_2-QDs.

MoS_2-QDs-AgNPs synthesized in one step chemical process have been visualized in TEM micrographs (Figure 5.3 a & b). AgNPs passivated by MoS_2-QDs prevent their agglomeration and account to its surface stabilization. This was further assured via elemental mapping shown in Figure 5.4. SAED pattern (Figure 5.3 c) similar to the hexagonal symmetry lattice of highly crystalline MoS_2-QDs and EDX spectrum (Figure 5.4) ensure its surface coverage over the AgNPs [Bai et al., 2017].

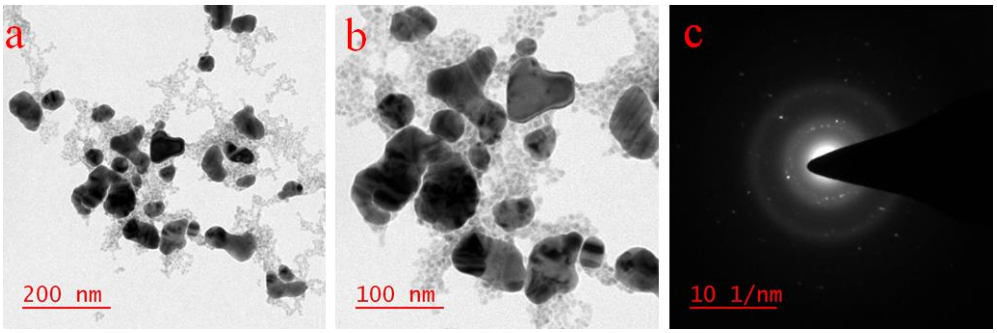

Figure 5.3 Characterization of MoS_2-QDs-AgNPs. TEM micrograph (a) at 200 nm scale bar (b) at higher resolution (100 nm) (c) SAED pattern.

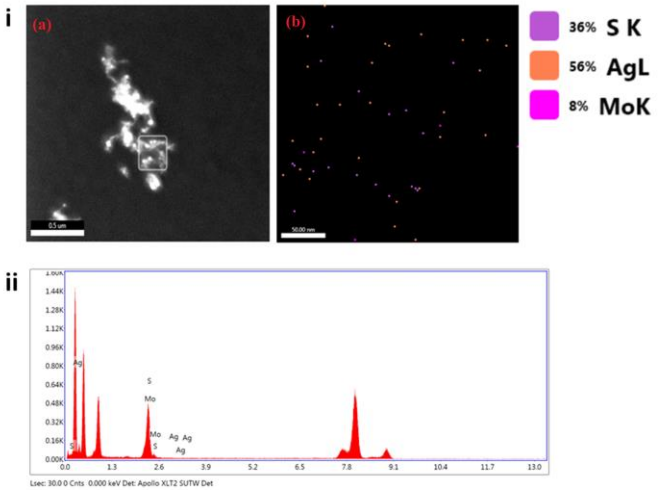

Figure 5.4 (i) (a) HAADF-STEM image and (b) elemental mapping of MoS_2-QDs-AgNPs. (ii) EDX spectrum of MoS_2-QDs-AgNPs.

MoS_2-QDs-AgNPs hydrosol stability was further investigated through its zeta potential measurement shown in Figure 5.5. The synthesized AgNPs were found to be stable for more than four weeks without any signs of aggregation. Zeta potential results are an average of 3 consecutive measurements done at room temperature. Both MoS_2-QDs and MoS_2-QDs-AgNPs exhibited consistent results with the variation of ±2 mV when checked at an interval of 7 days for 4 weeks. As shown, MoS_2-QDs and MoS_2-QDs-AgNPs exihibited similar (-30.8 and -32.8 mV respectively) zeta potential, thus supporting the surface coverage of MoS_2-QDs over AgNPs. The negative charge on the sulphur of QDs gives rise to electrical double layer formation that leads to the generation of repulsive forces between AgNPs resulting in its stable dispersion in the aqueous medium.

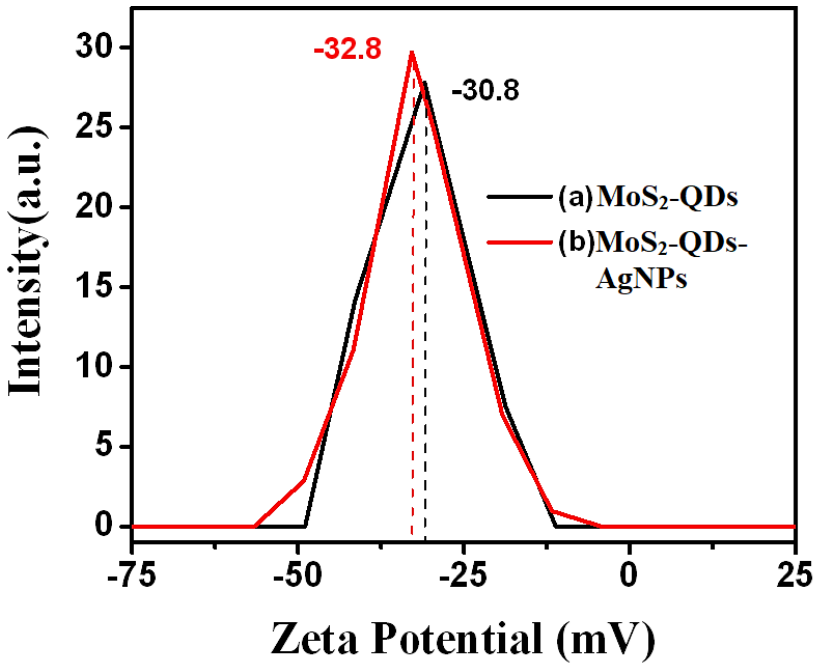

Figure 5.5. Zeta potential of MoS_2-QDs and MoS_2-QDs-AgNPs in aqueous medium.

The XPS spectrum of MoS_2-QDs (Figure 5.6 a) shows two strong peaks at 229.3 and 232.5 eV that correspond to Mo $3d_{5/2}$ and Mo $3d_{3/2}$ and at 226.6 eV which can be assigned to S 2s. XPS spectrum for the S 2p (Figure 5.6 b) shows the peak at 163.2 and 162.2 eV corresponding to the S $2p_{1/2}$ and S $2p_{3/2}$ orbital of divalent sulfide ions (S^{2-}) respectively [Eda et al., 2011, Li et al., 2016]. The binding energy peaks for Ag $3d_{5/2}$ (Figure 5.6 c) was observed at 368.0 eV as the characteristic peak for the metallic silver atoms of MoS_2-AgNPs and another peak with a binding energy of 369.4 eV can be assigned to the silver atoms bonded with sulphur atom (Ag–S). As splitting of the Ag 3d doublet is 6 eV, the peaks observed at 374.5 and 375.5eV can be attributed to Ag $3d_{3/2}$ of metallic silver atoms and silver atoms bonded to the sulphur (Ag–S) respectively [Matassa et al., 2012; Cheng et al., 2015]. Binding energy peak of Hg $4f_{7/2}$ and Hg $4f_{5/2}$ were obtained at 99.3 and 102.7 eV, indicating that it has been reduced to its elemental state (Figure5.6 d).

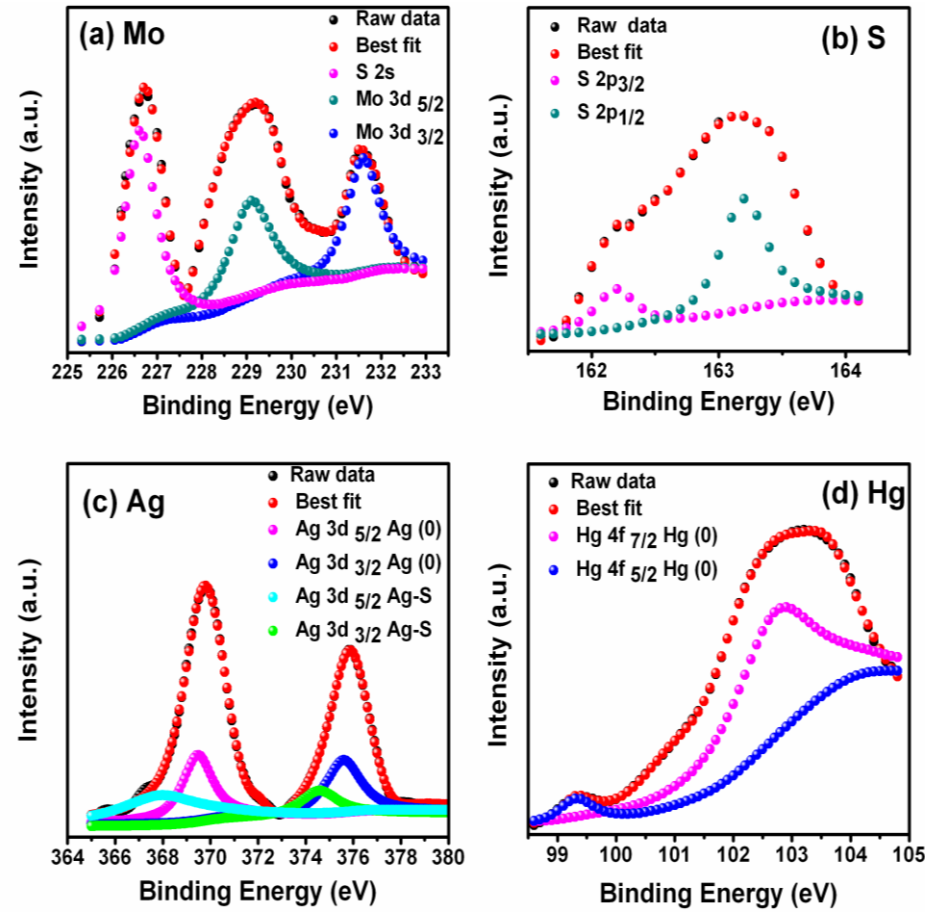

Figure 5.6. XPS spectra of (a) Mo 3d, (b) S 2p, (c) Ag 3d and (d) Hg 4f respectively.

5.3.2. Mercury(II) ion stimulated oxidase mimetic activity of MoS_2-QDs-AgNPs and inhibition by Cys.

Absorption spectra (Figure 5.7) displays TMB oxidation in presence of Hg^{2+} ion and MoS_2-QDs-AgNPs system. The characteristic absorptions of oxidized TMB occur at 370 and 652 nm furnishing intense blue color whereas the presence of alone Hg^{2+} (curve a) does not assist its oxidation. curve c shows no oxidation by MoS_2-QDs-AgNPs in absence of the Hg^{2+}. TMB catalytic activity inhibition is observed in presence of Cys (curve d) as compared to curve b. This dictates the complementary effect between MoS_2-QDs-AgNPs and Hg^{2+} ion towards TMB oxidation and corresponding inhibitory effect of Cys.

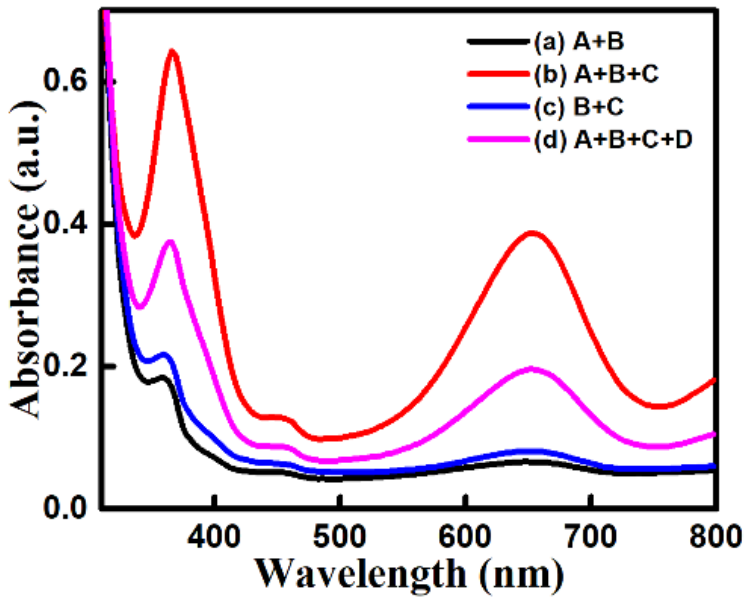

Figure 5.7. UV-vis spectra depicting TMB mimetic activity with various combinations (a) A+B, (b) A+B+C, (c) B+C, (d) A+B+C+D where A= Hg^{2+} (100 nM), B= TMB (1mM), C= MoS_2-QDs-AgNPs, D= Cys.

A schematic representing Hg^{2+} mediated TMB oxidase-like activity of MoS_2-QDs-AgNPs and the reaction principle is shown in Scheme 5.1. Hg^{2+}ion based colorimetric assay becomes possible due to the development of color as a result of the TMB oxidation in presence of MoS_2-QDs-AgNPs and O_2. Due to oxidase activity, Hg@MoS_2-QDs-AgNPs transfer the electrons to O_2 during the oxidation of the TMB and furnish blue color as a result of the formation of the charge transfer complex between oxidized and unoxidized TMB with a characteristic absorbance band at 652 nm. Cys has free thiol group that readily gets oxidized into csytine form due to formation of the disulfide bond in the presence of the nanozyme and O_2. This property of the Cys have inhibitory effect over the oxidase activity of Hg@MoS_2-QDs-AgNPs and results in no oxidation of the TMB. MoS_2-QDs aid in the formation of AgNPs and its surface stabilization in aqueous phase thus promoting electrostatic-ionic interactions with Hg^{2+} ion to form Ag-Hg solid amalgam (Hg@MoS_2-QDs-AgNPs) [Wang et al.,

2010; Mishra et al., 2017]. The reduction of Hg^{2+} and simultaneous deposition of Hg (0) on the surface of the NPs enhances its catalytic efficiency. Further, the Hg (0) deposition induces the aggregation of nanosystem that has been supported by TEM micrograph, EDX spectrum (Figure 5.8) and elemental mapping (Figure 5.9).

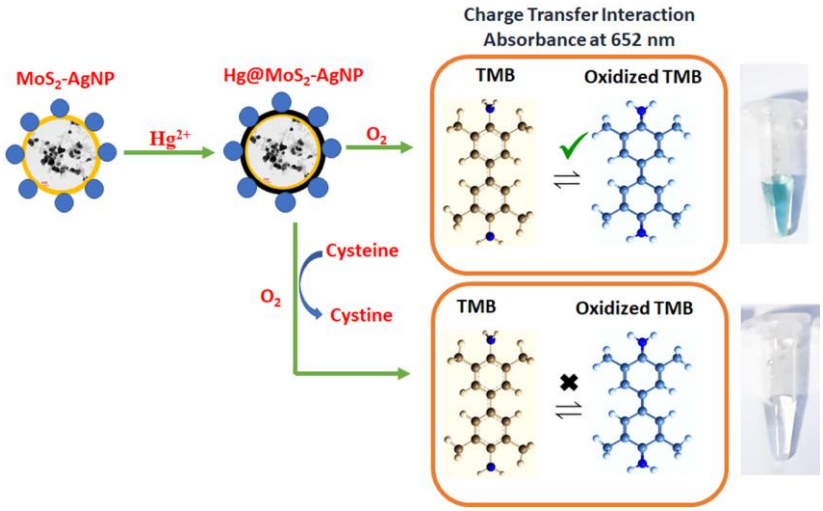

Scheme 5.1 Schematic representing Hg^{2+} mediated TMB oxidase like activity of MoS_2-QDs-AgNPs and the reaction principle for the colorimetric sensing of Cys.

XPS analysis, which is highly sensitive to the environments of the elements was additionally used to study the chemical composition of MoS_2-AgNPs and its interaction with Hg (shown in Figure 5.6 c and d). The presence of Hg (0) on the surface of MoS_2-QDs-AgNPs after its interaction with Hg^{2+} was also confirmed by XPS (Figure 5.6 d). These results along with TEM results (Figures 5.8 & 5.9) together, validate the interaction between AgNPs and Hg^{2+}.

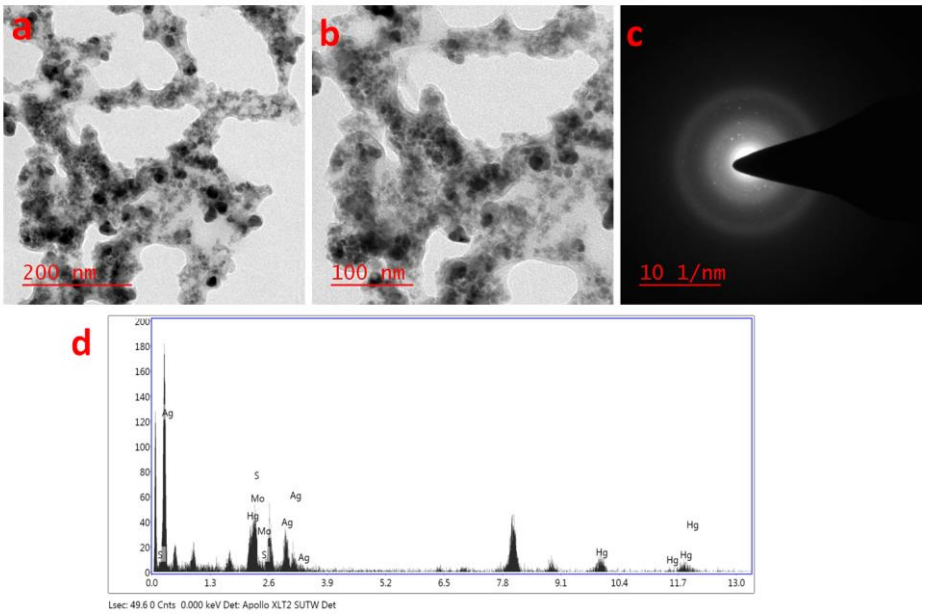

Figure 5.8. Investigation of interaction of Hg^{2+} with MoS_2-QDs-AgNPs. TEM micrograph (a) at higher scale bar (200 nm) (b) at lower scale bar (100 nm) (c) SAED pattern (d) EDX depicting elemental analysis.

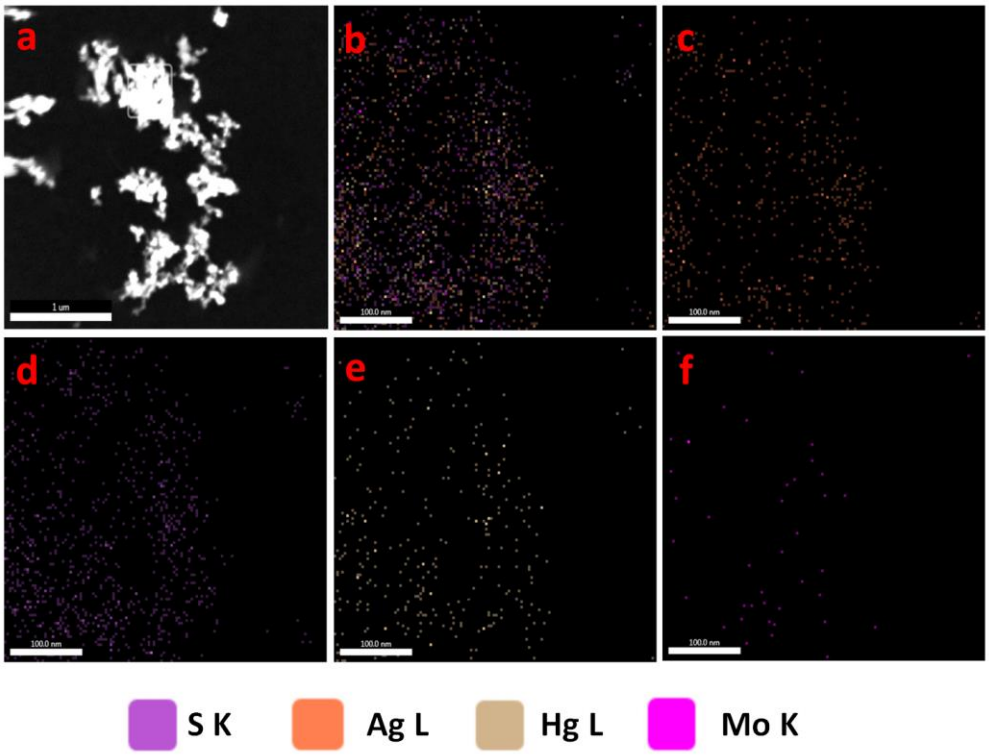

Figure 5.9. (a) HAADF-STEM image and (b) elemental mapping of MoS_2-QDs - AgNPs amalgation (c) S, (d) Ag, (e) Hg and (f) Mo.

5.3.3. Optimizations of parameters

Various parameters affecting TMB oxidation such as time (Figure 5.10 a), pH (Figure 5.10 b) and temperature (Figure 5.10 c) were optimized. Time-dependent study reveals excellent catalytic efficiency of Hg@MoS_2-QDs-AgNPs nanohybrid with colorimetric response produced within 10 min. Temperature and pH being the two most important parameters, significantly affect the catalytic efficiency of nanozyme. Temperature optimization of nanozyme shows its increasing catalytic activity up to 30^oC with active range from room temperature to 40 ^oC. The nanozyme exhibits maximum activity at pH 4.0. This is consistent with earlier reports [Gao et al., 2007; Wang et al., 2014]. It should be pointed out that Hg@MoS_2-QDs-AgNPs exhibited better stability in comparison to HRP and can work over a wider range of temperature.

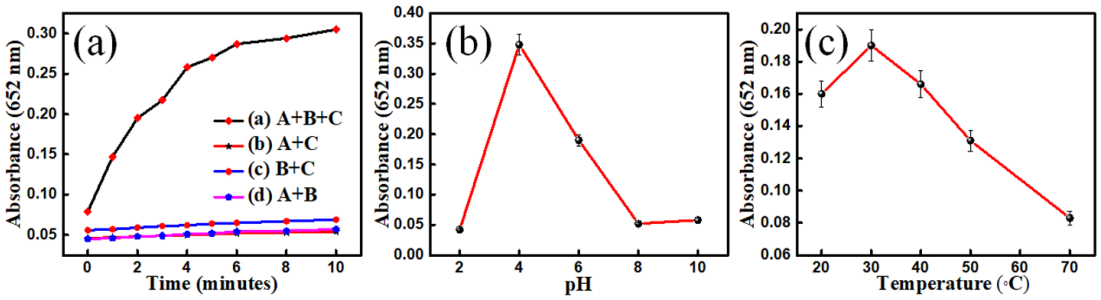

Figure 5.10 (a) Kinetic study of various combinations (i) A+B+C, (ii) A+B, (iii) A+C, (iv) B+C where A= Hg^{2+} (100 nM), B= TMB (1mM), C= MoS_2-QDs-AgNPs. Optimization of (b) temperature and (c) pH.

5.3.4. Enzyme kinetics study

Enzyme kinetics of Hg@MoS_2-QDs-AgNPs that depends on TMB concentration was studied by fixing all of them except TMB. As clearly observed from curves Figure 5.11 a & b, MoS_2-QDs-AgNPs follow Michaelis-Menten kinetics that can be expressed in the form of Michaelis-Menten equation (Eq.5.1) where υ_0 is the initial velocity, [S] is

the substrate concentration, V_{max} is maximum velocity and K_m is Michaelis–Menten constant (substrate concentration (S) at (V_{max})/2).

$$\upsilon_0 = (V_{max}\,[S]) / (K_m + [S]) \qquad (5.1)$$

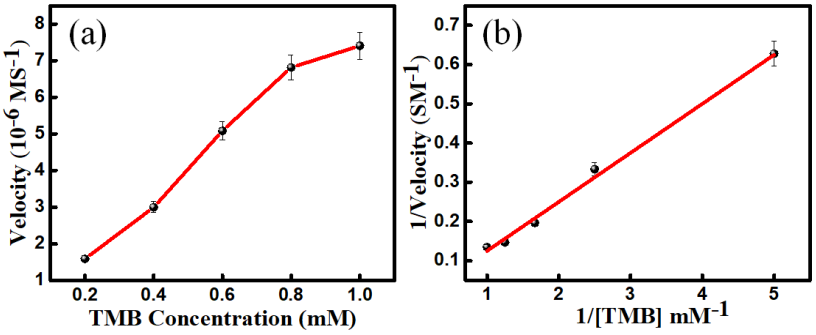

Figure 5.11 Enzyme kinetics study of (a) TMB concentration dependent (constant amount of Hg^{2+} and MoS_2-QDs-AgNPs in 0.2 M acetate buffer (pH=4.0)), (b) Lineweaver-Burk plot.

Figure 5.11 a shows the increase in enzymatic velocity with an initial increase in the concentration of TMB but saturates after a certain value. The optimum concentration of TMB was found to be 1 mM. K_m and V_{max} were found to be 390 μM and 7×10^{-6} MS^{-1} respectively for Hg@MoS_2-QDs-AgNPs. The smaller K_m value and greater V_{max} of Hg@MoS_2-QDs-AgNPs in comparison to HRP for TMB oxidation indicate better binding affinity towards substrates and enhanced catalytic efficiency due to the higher surface area allowing more interaction between MoS_2-QDs-AgNPs and TMB molecules in presence of the Hg^{2+} [Lu et al., 2016].

5.3.5. Colorimetric sensing of Cys

Futher on addition of Cys, the catalytic activity of the nanozyme (Hg@MoS_2-QDs-AgNP) is adversely affected and we get color contrast with increasing Cys concentration. The characteristic absorbance peaks of oxidized TMB occurring at 370 and 652 nm in presence of MoS_2-QDs-AgNPs and Hg^{2+} exhibits fading intensity with

varying Cys concentration (1μM to 100 μM). This inhibitory effect of Cys is clearly visible visually color differences (inset of Figure 5.12 a). Figure 5.12 b shows a linear calibration plot for Cys concentration. The experiment was repeated 10 times and plotted after taking an average. Limit of detection (LOD) was found to be 824 nM that was derived from the expression LOD = $(3*S_d)$/slope.

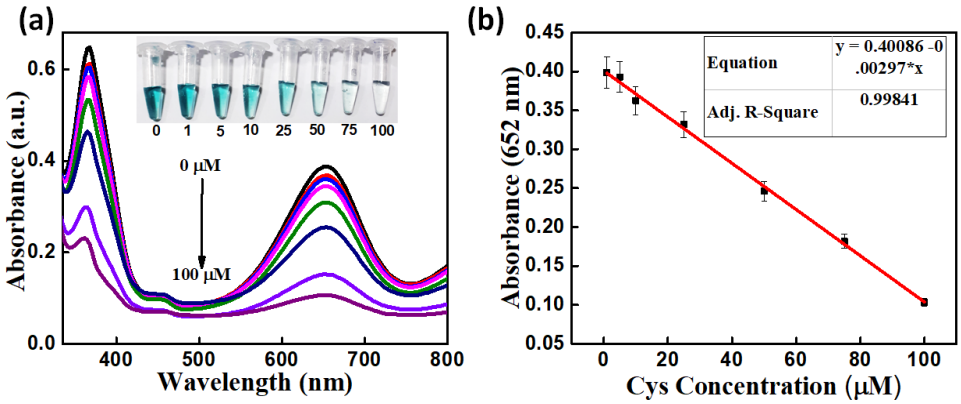

Figure 5.12. (a) UV-vis spectra depicting TMB mimetic activity with varying concentration of Cys (a) 0 (b) 1 (c) 5 (d)10 (e) 25 (f) 50 (g) 75 (h) 100 μM. Inset showing the real pictures with difference in color intensity with varying concentration. (b) Linear calibration plot for Cys detection.

5.3.6. Reproducibility

MoS_2-QDs-AgNPs mimetic activity for catalytic TMB oxidation in Hg^{2+} presence for the Cys detection was repeated on hourly and daily basis to investigate the reproducibility of results. The identical experiments were performed many times at an interval of 3 hours in a day (i.e. 0, 3, 6, 9 ,12 hours) and repeated over four days with the same concentration range of Cys (1-100 μM and intra-day (Figure 5.13 a). Inter-day (Figure 5.13 b) study plots reveal that catalytic activity of Hg@MoS_2-QDs-AgNPs is highly reproducible over time. These comparable results very well validate the reproducibility as well as the stability of the Hg@MoS_2-QDs-AgNPs.

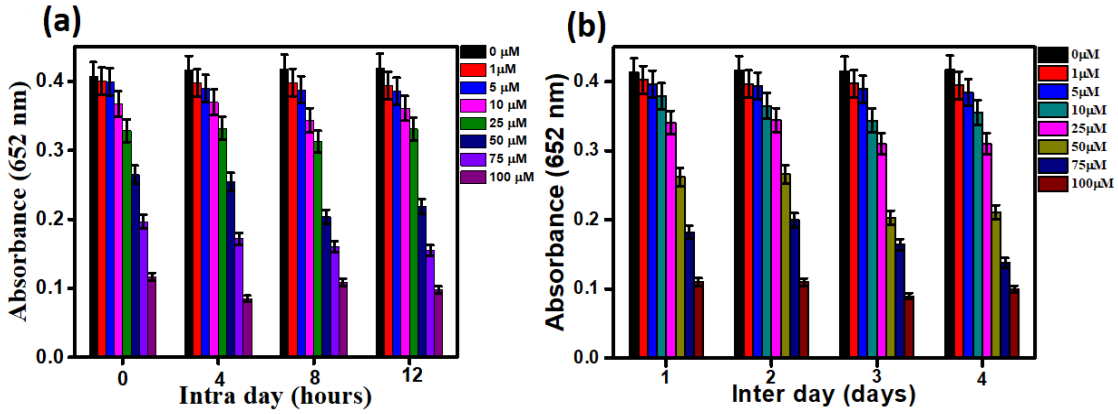

Figure 5.13. (a) Intra-day and (b) inter-day study for catalytic activity of Hg@MoS_2-QDs-AgNPs towards TMB oxidation.

5.3.7. Selectivity and interference study for Cys

To demonstrate the selectivity of the Cys, absorbance spectra were recorded at 652 nm for enzyme mimetic activity of Hg@MoS_2-QDs-AgNPs in presence of various amino acids such as Gly, Ala, Leu, Glu, Trp, Pro, Met, His, Tyr, Asp, Glu, GSH, Cys and HCys. Although concentrations of other amino acids were 10 fold greater except GSH and HCys, Cys exhibited significantly larger inhibition effect (Figure 5.14) that indicates Hg@MoS_2-QDs-AgNPs possesses selectivity towards Cys.

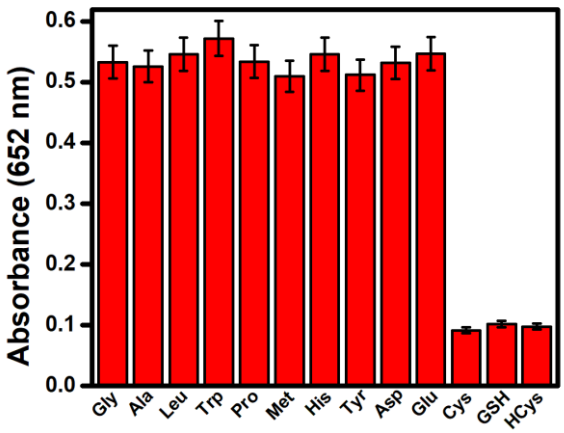

Figure 5.14 Selectivity of various aminoacids towards Hg@MoS_2-QDs-AgNPs and their interference study.

5.3.8. Real sample analysis

The feasibility of Hg@MoS_2-QDs-AgNPs nanozyme catalytic activity was also investigated in the blood serum obtained from human. For this purpose, colorimetric signals of blood serum (30 times diluted) spiked with various Cys concentrations (0, 1, 5, 10, 25, 50, 75, 100 μM) were recorded as shown in Figures 5.15 a & b. The spectra shows significant decrease in the absorbance with increase in the Cys concentration. The obtained spectra depicts good linearity with regression coeffficent of 0.976 and limit of detection as 7.7 μM calculated using expression LoD = (3*SD)/slope. Table 5.1 shows good recoveries (from 90 % to 109%) of the known amount Cys in real samples that supports the reliability of the method in the biological sample.

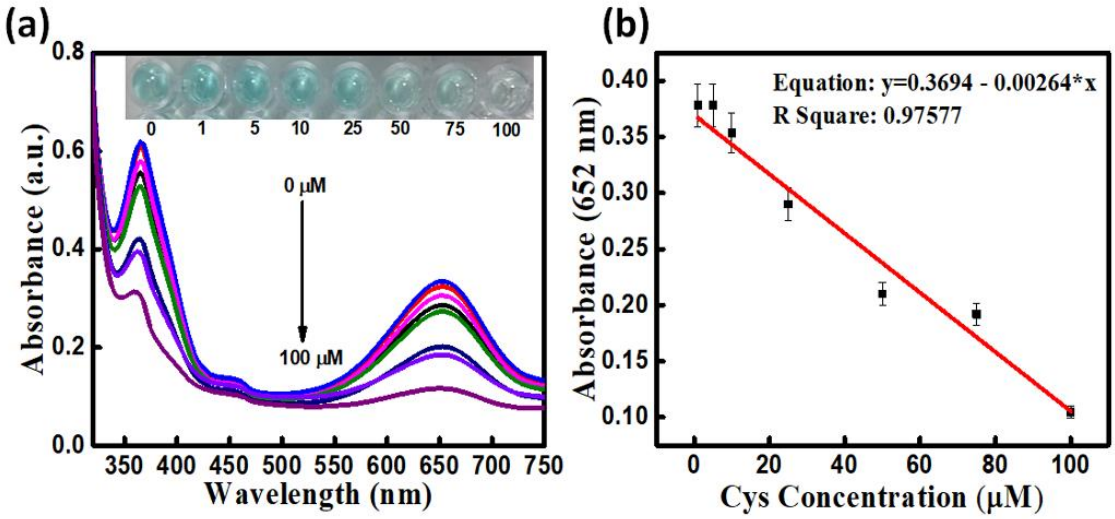

Figure 5.15. Real sample analysis in human blood serum spiked for Cys. (a) UV-vis spectra showing TMB mimetic activity with varying Cys concentration i.e. 0, 1, 5, 10, 25, 50, 75 and 100 μM in blood serum. Inset showing the real pictures with color intensity difference with concentration. (b) Linear calibration plot for Cys detection in blood serum.

Table 5.1: Recovery study and determination of Cys in the blood serum.

S.No.	Added Cys(μM)	Found Cys(μM)	Recovery(%)
1	**25**	**27.3**	**109**
2	**50**	**54.2**	**108**
3	**75**	**67.5**	**90**

Table 5.2: Comparison of the sensitivity and linearity for Cys in recent methods.

Material	Method	LoD	Advantage	Range of response (μM)	Ref.
DNA-Ag/Pt nanoclusters	Colorimetry	2 nM	High sensitivity	0-0.500×10^{-6}	**[Wu et al., 2016]**
Ag^{+} -TMB	Colorimetry	2.46 μM	Simple & selectivity	2.0×10^{-6} - 100×10^{-6}	**[Xue et al., 2019]**
Fe^{3+}–TMB–H_2O_2	Colorimetry	0.97 μM	Stability & Selectivity	0 - 50×10^{-6}	**[Wu et al., 2014]**
$Gd(OH)_3$ nanorods.	Colorimetry	2.6 μM	Selectivity & precision	0.2×10^{-6}-400×10^{-6}	**[Sing et al., 2017]**
Hg@MoS_2-QDs-AgNPs	**Colorimetry**	**824 nM**	**High sensitivity and selectivity; instrument free**	**1.0×10^{-6} - 100 ×10^{-6}**	**This work**

Based on some previous reports for colorimetric detection assay we have prepared Table 5.2 enlisting the recent approaches towards Cys sensing. Table 5.2 clearly

demonstrates our work comparable to other used nanozymes on the basis of selectivity, LOD, reproducibility, time-saving and most importantly on economic ground.

5.3.9. Portable test kit for Cys detection in real sample

We have developed a portable plastic tubes based device (Figure 5.16) that can be used for naked eye detection of Cys. Prior to colorimetric sensing, device was developed through steps: agarose water suspension (20 $g.L^{-1}$) was boiled for 10 min and then left for cooling down to room temperature. After that 100 µL of Hg@MoS_2-QDs-AgNPs containing 1 mM Hg^{2+} was added to it with vigorous stirring. Then this mixture was added to the cap of the plastic tubes and preserved in cool and dark condition for gel formation and to avoid any oxidation. Then after, test samples (100 µL) having different Cys concentrations (0-100 µM) and TMB buffer (100 µL) were added to the plastic tubes and kept for 20 min in the inverted position (Figure 5.16 a). Blue color contrast was observed with increasing Cys concentration as shown in Figure 5.16 c, based on which we developed a color scale (wheel) that shows different shades of blue corresponding to various Cys concentration level (Figure 5.16 b). This color wheel chart may be highly useful for quick detection of Cys in field analysis.

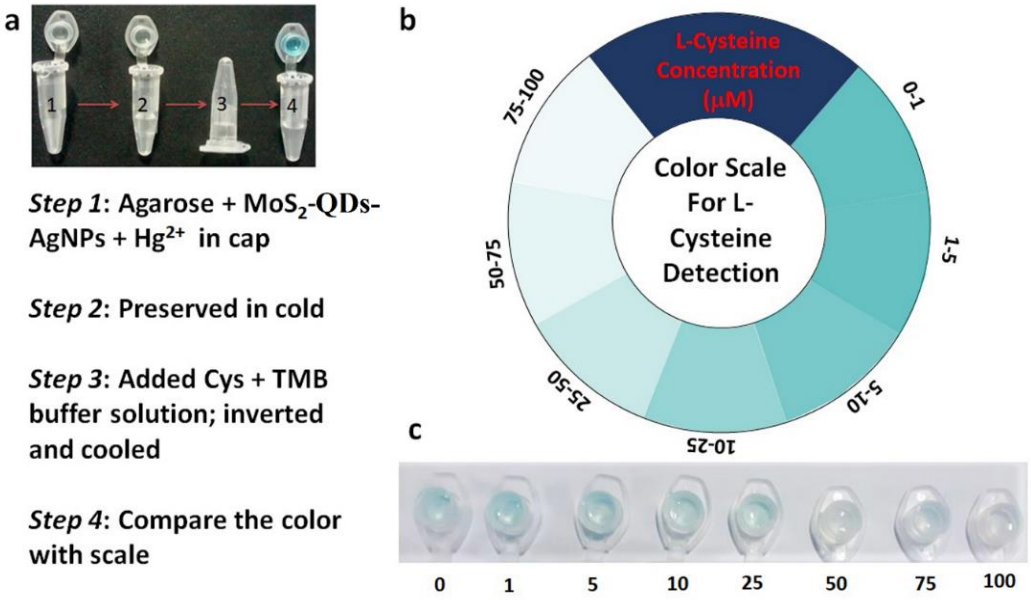

Figure 5.16. Plastic tubes kit based colorimetric detection. (a) Image showing the process to use kit. (b) Color scale wheel chart developed to check the Cys level (μM) (c) photograph showing the response of kit to various concentrations (in μM) of Cys.

5.4. CONCLUSION

In summary, we have successfully demonstrated highly efficient and sensitive colorimetric sensing platform for the detection of Cys in real sample (blood serum), utilizing robust oxidase mimetic activity of MoS_2-QDs stabilized AgNPs stimulated by Hg^{2+}. The developed sensor for Cys detection exhibited wide dynamic range 1-100 μM with lower detection limit of 824 nM. The most astonishing feature of this work is the quick ultra-trace level detection of Cys aided with cost-effective plastic tubes based kit. This approach utilizing the synergistic effect of MoS_2-QDs-AgNPs and Hg^{2+} towards enhancement in catalytic efficiency of the system may prove to be economically beneficial for quick and easy detection of Cys. The presented assay is an efficient, simple, cost-effective, sensitive and applicative within the clinical health range for accurate identification of Cys.